Single-Optimization of Ultrasonic Vibration-Assisted EDM for External Cylindrical Machining of 90CrSi

Van Thanh Dinh
East Asia University of Technology, Trinh Van Bo Street, Hanoi City 12000, Vietnam
thanh.dinh@eaut.edu.vn

Thu Quy Le
National Research Institute of Mechanical Engineering, 04 Pham Van Dong, Ha Noi City 11309, Vietnam
quylt@narime.gov.vn

Thi Tam Do
Thai Nguyen University of Technology, 3/2 street, Tich Luong ward, Thai Nguyen City 251750, Vietnam
dothitam@tnut.edu.vn

Ngoc Pi Vu
Thai Nguyen University of Technology, 3/2 street, Tich Luong ward, Thai Nguyen City 251750, Vietnam
vungocpi@tnut.edu.vn

Thi Phuong Thao Tran
Thai Nguyen University of Technology, 3/2 street, Tich Luong ward, Thai Nguyen City 251750, Vietnam
tranphuongthao@tnut.edu.vn (corresponding author)

Received: 12 April 2025 | Revised: 7 May 2025 and 25 May 2025 | Accepted: 27 May 2025

 DOI: https://doi.org/10.48084/etasr.11450

ABSTRACT

The present study investigates the optimization of Ultrasonic Vibration-Assisted Electrical Discharge Machining (UV-EDM) for external cylindrical machining of 90CrSi tool steel, a material known for its high hardness and poor machinability by conventional methods. Traditional EDM often suffers from low Material Removal Rate (MRR) and poor surface finish (Ra), limiting its productivity and surface integrity. To address this, the research aims to determine optimal machining parameters that enhance MRR while maintaining or improving Ra using ultrasonic assistance. A Box–Behnken experimental design was employed with five input parameters: vibration amplitude, pulse-on time, pulse-off time, discharge current, and servo voltage. Forty-six experiments were conducted, and second-order regression models were developed for both MRR and Ra. The effects and interactions of parameters were analyzed using response surface plots and interaction heatmaps. Results show that discharge current and pulse-on time strongly influence MRR, whereas servo voltage and pulse-off time significantly affect Ra. Ultrasonic vibration was found to notably increase MRR, and when properly tuned, improved surface roughness by enhancing debris evacuation and discharge stability. Key interaction effects (e.g., between current and amplitude) were identified, emphasizing the importance of balanced settings. The developed regression models (R^2 = 0.987 for MRR and R^2 = 0.783 for Ra) provide reliable predictions and can support future process control. Overall, UV-EDM proves to be a highly effective technique for improving both efficiency and surface quality in precision machining of hard tool steels.

Keywords-ultrasonic vibration-assisted EDM; single-objective optimization; 90CrSi tool steel; surface roughness; material removal rate; Box–Behnken Design (BBD); regression modeling

I. INTRODUCTION

Electrical Discharge Machining (EDM) is a highly effective technique for machining electrically conductive materials with high hardness and complex geometries that are difficult to process using conventional methods. However, EDM typically faces two major challenges: low Material Removal Rate (MRR) and high surface roughness (Ra), both of which negatively impact productivity and product quality [1, 2]. The study by authors in [3] emphasized that simultaneous optimization of Ra and MRR is necessary to enhance EDM performance. Similarly, authors in [4] developed predictive models for surface roughness indicators such as Ra and Rq when machining ceramics via EDM, demonstrating the significant influence of process parameters on surface quality.

In another line of research, authors in [5] highlighted the importance of post-EDM surface topography analysis to better understand the microstructural impacts of the process. In addition, the authors of [6] demonstrated that variations in discharge current and pulse duration significantly affect Ra, MRR, and electrode wear. Modeling of the EDM process has also received substantial attention. For instance, in [7], the authors applied Response Surface Methodology (RSM) to construct a regression-based predictive model for MRR.

In the context of optimization techniques, authors in [2] employed the Artificial Bee Colony (ABC) algorithm to perform multi-objective optimization of Ra and MRR when machining EN31 tool steel. Subsequently, the same research group expanded their study by employing the Weighted Principal Component Analysis (WPCA) approach [8], which yielded promising results in identifying optimal machining parameters.

More recently, Ultrasonic Vibration-Assisted Electrical Discharge Machining (UV-EDM) has gained significant interest as a means to enhance EDM performance. In [9], the authors reported that ultrasonic vibration substantially improves debris removal mechanisms. In a follow-up study, authors in [10] demonstrated that the vibration amplitude directly affects the accuracy and speed of micro-hole machining. In addition, authors in [11] employed UV-EDM to machine TiN ceramic and achieved significant improvements in machining characteristics. Beyond experimentation, authors in [12] performed Finite Element Method (FEM) simulations of UV-EDM and illustrated how ultrasonic vibrations influence energy distribution and material behavior.

The integration of UV-EDM with other technologies is a continually evolving field. In [13], the authors proposed a methodology involving the combination of ultrasonic vibration with silver powder-mixed EDM to fabricate surfaces with antibacterial properties. Authors in [14] observed bubble dynamics in the spark gap under ultrasonic vibration. Another advanced technique, Ultrasonic Circular Vibration (UCV), developed by authors in [15, 16], has proven effective in improving surface integrity and dimensional accuracy in micro-EDM applications.

Authors in [17] demonstrated the effectiveness of EDM in gas media when combined with ultrasonic vibration and Abrasive Jet Machining (AJM), offering new capabilities for delicate feature fabrication. As early as the 1990s, researchers in [18] demonstrated that synchronizing electrical pulses with ultrasonic vibrations could significantly boost machining efficiency. Finally, authors in [19] confirmed that the combination of ultrasonic vibration and micro-powder suspension in the dielectric enhances both surface quality and material removal performance.

Recent studies have continued to explore the optimization of EDM processes for different materials. In [20], the authors implemented a Multi-Criteria Decision-Making (MCDM) approach to identify the optimal input factors for EDM of 90CrSi tool steel using graphite electrodes. The authors emphasized the material's industrial relevance and sensitivity to process parameters. Their findings highlighted the strong influence of pulse-on time and current on both MRR and Ra, reinforcing the need for precise control in EDM of hard steels. In another recent work, authors in [21] investigated the effect of EDM settings on surface roughness and electrode wear when machining 7024 aluminum alloy. Their results confirmed that improper parameter selection can significantly degrade surface integrity and accelerate tool erosion, even for soft alloys. This finding further underscores the challenge of process control in EDM.

Based on these prior studies, it is evident that single-objective optimization aimed at either minimizing surface roughness or maximizing material removal rate in UV-EDM processes is both timely and practically relevant. The present study focuses on the construction of a predictive model for single-objective optimization in UV-EDM, with the goal of significantly enhancing EDM performance by leveraging the superior characteristics of ultrasonic vibration.

II. METHODOLOGY

The development of a statistically reliable and computationally efficient Design of Experiments (DOE) approach is essential for effectively modeling the influence of multiple process parameters on the performance of UV-EDM. In this study, the Box–Behnken Design (BBD) was selected due to its balance between experimental economy and its ability to model nonlinear relationships, including second-order interactions, without requiring an excessive number of experimental runs.

Compared to Taguchi designs, which are primarily suited for robust parameter design and emphasize main effects over interactions, BBD provides greater flexibility for Response Surface Modeling (RSM) when significant curvature or interaction effects are expected between variables. Moreover, while full factorial or Central Composite Designs (CCDs) offer comprehensive coverage of the factor space, they require a substantially larger number of runs, which may be impractical for complex processes like EDM that are time- and resource-intensive. In contrast, BBD places experimental points at the midpoints of the edges and at the center of the design space.

This approach avoids extreme corner combinations that may be infeasible or unstable in EDM applications, particularly those involving ultrasonic vibration [22].

A key criterion in selecting BBD for this study was the desire to limit the total number of experiments to under 50, thereby ensuring sufficient model accuracy while keeping the experimental workload and cost within practical limits. With five independent variables, the BBD generated 46 experimental runs, including center-point replications for estimating experimental error. This number was determined to be suitable for capturing the essential interactions and quadratic effects while maintaining statistical reliability [23].

The experimental design involved five input variables: ultrasonic vibration amplitude (A), pulse-on time (Ton), pulse-off time (Toff), discharge current (IP), and servo voltage (SV). Each of these variables was varied at three coded levels: −1, 0, and +1. The two output responses evaluated were material removal rate MRR (g/h) and Ra (µm).

The entire experimental matrix was randomized to minimize systematic bias and ensure the robustness of statistical inference. Subsequent data analysis involved the construction of second-order regression models, interaction matrices, main effects plots, contour maps, and 3D response surfaces to uncover both individual and synergistic influences of the process parameters.

III. EXPERIMENTAL WORK

A. Experimental Setup and Materials

The machining experiments were performed on a custom-configured UV-EDM system (Figure 1), where the ultrasonic vibration module operated at a constant frequency of 20 kHz. The workpiece material was 90CrSi tool steel, known for its high hardness and wear resistance, and was heat-treated to a final hardness range of 58–60 HRC.

The chemical composition of the workpiece material is presented in Table I. Commercially pure copper was used as the tool electrode in all trials, whereas Diel MS 7000 dielectric fluid was employed to ensure adequate flushing and thermal stability during machining. Table II presents the experimental plan.

B. Procedure for Measuring Material Removal Rate

MRR was determined gravimetrically using the weight-loss method, a standard approach in EDM performance evaluation. The procedure involved the following steps:

- Each workpiece was cleaned with ethanol, dried with warm air, and weighed using a precision electronic balance with 0.1 mg accuracy prior to machining.
- After machining under the specified EDM conditions, the sample was again cleaned and reweighed.
- The MRR was then calculated by dividing the mass loss by the machining time in hours:

$$\mathrm{MRR} = \frac{m_{before} - m_{after}}{t} \quad (1)$$

In all trials, commercially pure copper was utilized as the tool electrode. The variables m_{before} and m_{after} denote the sample masses before and after machining, respectively, whereas t is the machining time in hours.

TABLE I. CHEMICAL COMPOSITION OF 90CRSI TOOL STEEL

Element	C	Cr	Si	Mn
Composition	0.85–0.95	0.90–1.20	0.40–0.60	≤0.40
Element	P (max)	S (max)	Fe	
Composition	≤0.030	≤0.030	Balance	

TABLE II. EXPERIMENTAL PLAN AND OUTPUT RESULTS

Trial	**A (µm)**	**Ton (µs)**	**Toff (µs)**	**IP (A)**	**SV (V)**	**MRR (g/h)**	**Ra (µm)**
1	1.15	12	12	5	5	3.374	4.028
2	1.15	16	12	7	5	5.004	7.031
3	1.15	8	12	3	5	1.086	2.335
4	1.15	12	12	3	7	1.994	2.635
5	1.6	12	12	3	5	0.836	3.294
6	1.15	16	12	3	5	1.191	3.538
7	1.15	8	8	5	5	1.493	2.487
8	1.15	16	8	5	5	3.354	5.773
9	1.15	8	12	5	7	1.417	3.190
10	1.15	8	16	5	5	1.360	3.050
11	1.15	12	12	5	5	3.292	4.023
12	1.15	12	8	5	3	3.546	3.770
13	1.15	12	12	7	3	3.729	5.172
14	1.15	16	16	5	5	3.098	3.850
15	1.15	12	12	5	5	3.275	4.018
16	1.75	12	12	7	5	2.542	3.560
17	1.15	12	12	5	5	3.249	4.015
18	1.15	12	8	5	7	3.349	3.550
19	1.6	16	12	5	5	1.972	3.555
20	1.6	12	8	5	5	2.506	3.580
21	1.75	12	12	5	7	1.669	3.610
22	1.15	8	12	7	5	1.392	3.190
23	1.75	8	12	5	5	0.305	2.687
24	1.6	12	16	5	5	2.373	3.760
25	1.15	12	8	7	5	4.054	5.200
26	1.15	12	16	5	3	3.252	3.755
27	1.15	12	12	5	5	3.313	4.026
28	1.15	12	8	3	5	1.996	3.787
29	1.15	16	12	5	3	2.947	3.530
30	1.15	16	12	5	7	3.517	3.780
31	1.15	12	16	7	5	3.736	4.720
32	1.15	12	16	5	7	3.202	4.770
33	1.75	12	16	5	5	2.156	4.790
34	1.15	12	12	7	7	3.609	4.710
35	1.75	12	8	5	5	2.322	4.300
36	1.6	12	12	7	5	2.720	4.441
37	1.15	8	12	5	3	1.349	3.010
38	1.15	12	12	5	5	3.390	4.031
39	1.6	12	12	5	7	2.210	4.740
40	1.75	16	12	5	5	1.828	3.540
41	1.6	8	12	5	5	0.361	2.675
42	1.6	12	12	5	3	2.372	4.210
43	1.15	12	12	3	3	1.275	3.161
44	1.75	12	12	3	5	0.916	3.785
45	1.15	12	16	3	5	1.914	3.685
46	1.75	12	12	5	3	2.034	4.116

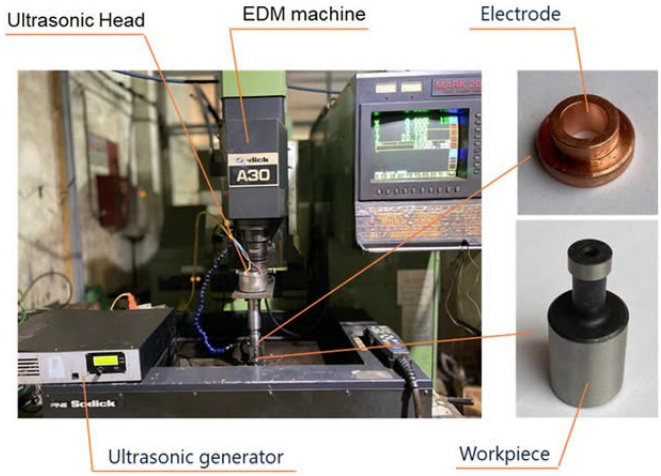

Fig. 1. Experimental setup.

C. Procedure for Measuring Surface Roughness

Surface roughness (Ra) was measured in accordance with ISO 4287 using the SV-3100 surface roughness tester (manufactured by Mitutoyo, Japan), which is capable of providing consistent, high-resolution measurements in the micrometer range. To account for spatial variability in surface texture, each sample was measured at three different locations on the machined surface. The final Ra value for each experiment was obtained by calculating the arithmetic mean of the three readings, which provides a more statistically robust estimate of surface finish.

All measurements were conducted in a controlled laboratory environment to eliminate environmental variations such as humidity, vibration, or thermal drift, which could affect precision.

IV. RESULTS AND DISCUSSION

A. Effects on Material Removal Rate

The MRR showed clear dependence on the EDM input parameters. As depicted in the main effects plot (Figure 2), the discharge current (IP) is the dominant factor influencing MRR. Increasing the peak current greatly boosts MRR due to the higher discharge energy per pulse, a trend widely reported in EDM studies [24]. For example, raising IP from its low to high setting led to the largest jump in MRR among all factors depicted in Figure 2. Pulse-on time (Ton) and vibration amplitude (A) are the subsequent most significant factors. A longer pulse duration and a higher amplitude cycle (i.e. a shorter pulse-off, Toff) both contribute to increased material removal. With a longer Ton, each discharge has more time to erode material, and with a higher vibration amplitude (more frequent pulses), the number of discharges per second increases. Both effects result in an elevation of the MRR. This is evident in the contour plot of MRR (Figure 3) for A vs. Ton, where the upper-right region (high amplitude, long pulse) yields the highest MRR. Conversely, a reduction in Toff, which corresponds to an increase in amplitude, results in a shift of the operating point toward higher MRR. However, it should be noted that extremely short off-times can compromise stability. Servo voltage (SV) also plays a role since a moderate increase in SV improved MRR by reducing the incidence of short-circuiting at too small a gap, as seen by the rising MRR trend with SV in Figure 3 (right contour plot of IP vs. SV). At very high SV, however, the gap may become too large, resulting in a slight reduction in discharge frequency. In our results, MRR peaked at an intermediate SV. The 3D surface plot (Figure 4) further illustrates these relationships, showing a pronounced MRR peak at the combination of high IP and high vibration amplitude. Overall, all five inputs exhibit physically intuitive effects on MRR. Higher energy input (via IP and Ton) and higher pulse frequency (via A and appropriate SV) lead to higher material removal, whereas long pulse-off times or insufficient gap voltage limit the discharge frequency and lower MRR.

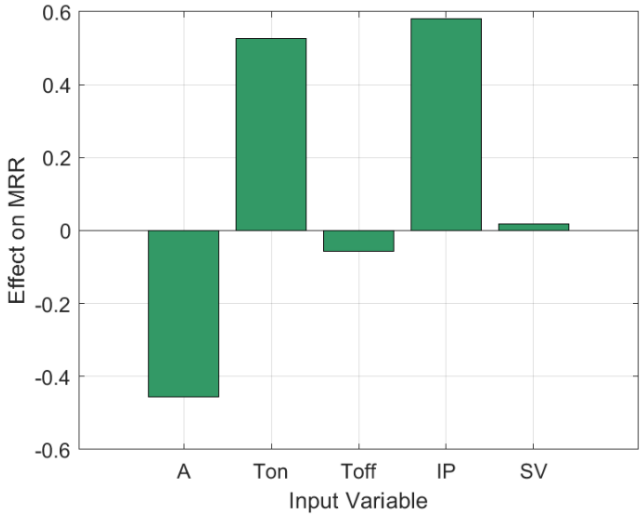

Fig. 2. Effect of input parameters on MRR.

Notably, the application of ultrasonic vibration in the EDM process markedly enhanced the achieved MRR under all parameter combinations. The ultrasonic assistance improves the flushing of debris and stabilizes the discharge, effectively allowing the process to capitalize on aggressive settings like high current or high amplitude without the usual penalty of arcing. This is consistent with prior research that demonstrated ultrasonic vibration can significantly increase MRR by promoting more efficient debris removal [25]. The cavitation bubbles and micro-jetting action induced by ultrasonic oscillations continually clear the spark gap [25], leading to a higher effective discharge frequency and thus higher MRR. In fact, literature suggests that introducing ultrasonic vibration can improve MRR by tens of percent compared to conventional EDM [25]. Our results support this finding: the maximum MRR observed with ultrasonic vibration is substantially higher than what would be expected without vibration, under comparable electrical parameters. This improvement in MRR is in line with the 70% increases reported by others for ultrasonic-assisted EDM [25], reaffirming that ultrasonic vibration is an effective means to overcome the low throughput of traditional EDM.

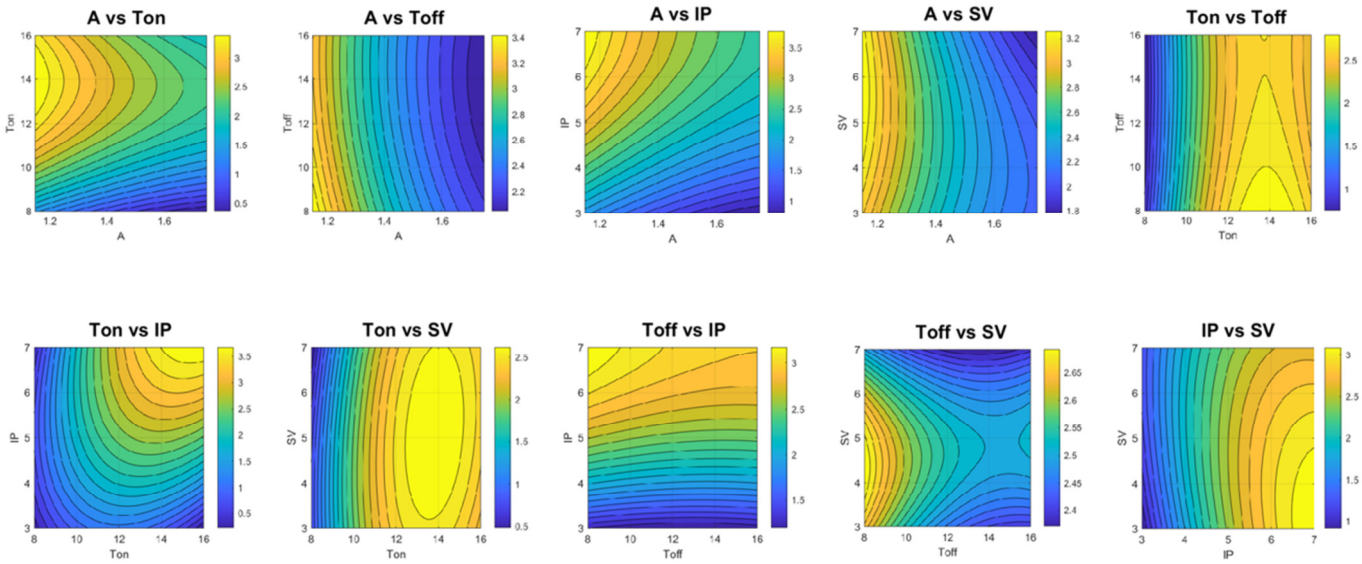

Fig. 3. Contour plots of input parameters on MRR.

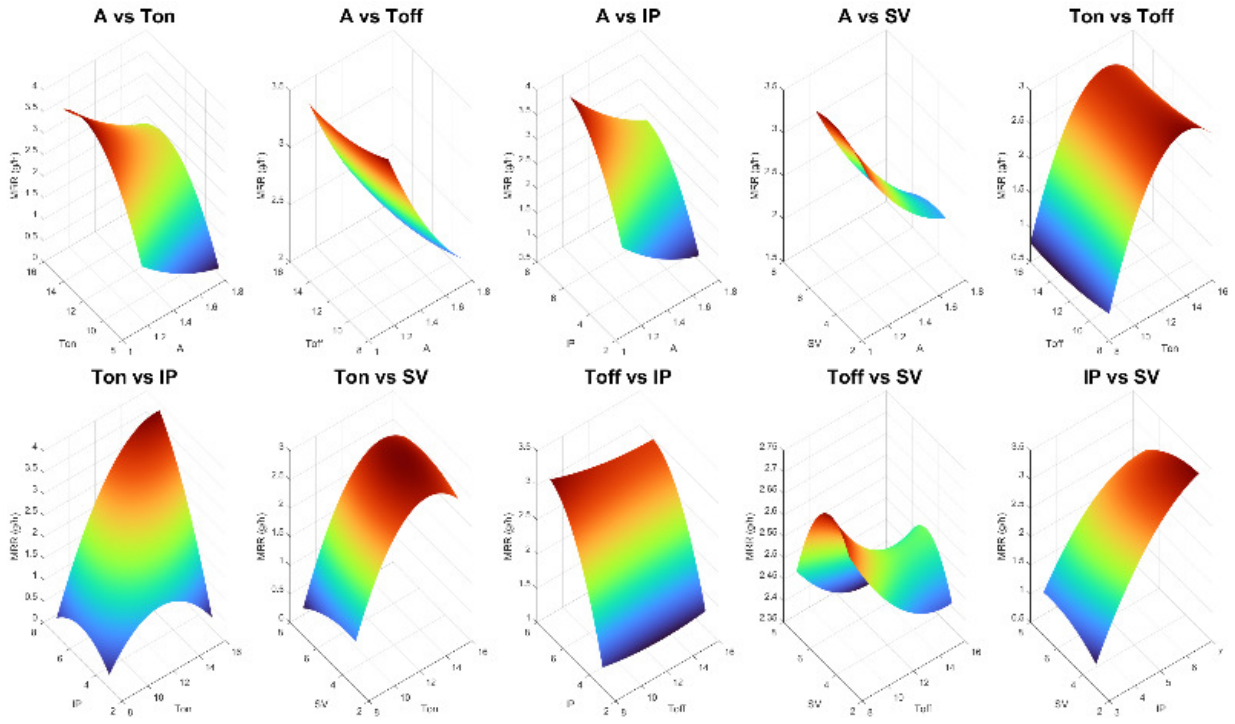

Fig. 4. 3D surface plots of input parameters on MRR.

B. Effects on Surface Roughness

The surface roughness (Ra) of the machined samples was found to be largely influenced by the same energy-related factors yet exhibited opposite trends in terms of enhancing surface quality. As illustrated in Figure 5, the discharge current has a pronounced effect on surface finish, with higher IP producing a rougher surface (higher Ra) due to the more violent sparks and larger craters formed on the workpiece. Pulse-on time exhibits a similar trend, with longer Ton resulting in a deterioration of the surface finish due to the enlargement of discharge craters and an increase in heat input per spark, consequently raising Ra [24]. For instance, as Ton increased from its low to high level in our experiments, Ra climbed markedly (Figure 5), consistent with the observation that extended discharge duration yields larger molten zones and resolidified craters [24]. These results align with the findings of previous studies, demonstrating that enhancing pulse energy (via current or on-time) leads to higher surface roughness [24]. In the contour plot of Ra (Figure 6), this appears as a region of high roughness at the conditions of high IP and long Ton (upper-right of the contour).

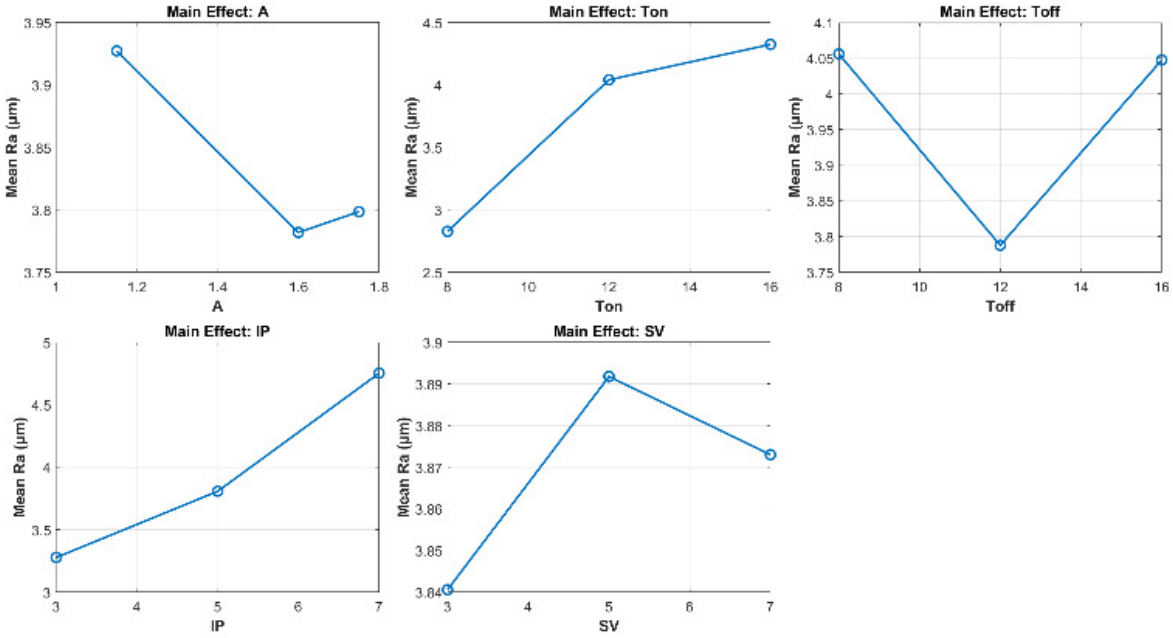

Fig. 5. Main effects plots for Ra.

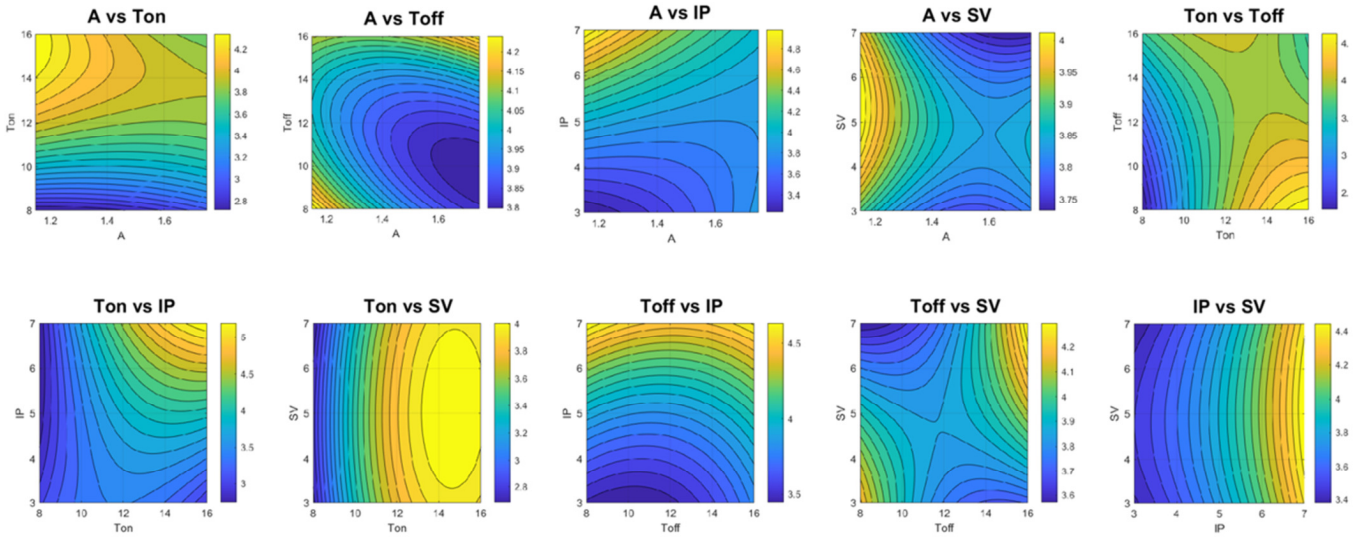

Fig. 6. Contour plots of input parameters on Ra.

On the other hand, parameters that improve stability and reduce discharge density tend to improve the surface finish (lower Ra). Increasing the pulse-off time has a beneficial effect on Ra: a longer Toff (lower vibration amplitude) allows for more cooling and flushing between discharges, which in turn diminishes overlapping crater damage on the surface. Thus, Ra decreases as Toff increases (or equivalently, Ra increases when vibration amplitude A is too high). This trend is visible in Figure 4, where the Ra is observed to be at its minimum at the maximum Toff setting. This finding aligns with reports indicating that incorporating a longer pause between pulses facilitates the solidification of molten material and enables the evacuation of debris, thereby producing a smoother surface [24]. Furthermore, it was determined that servo voltage significantly affects surface quality. As the servo voltage setting was increased, the average gap widened slightly, which prevented very close-contact discharges and unstable arcing. The result was a noticeable improvement in Ra, with higher SV. Figure 4 illustrates Ra decreasing as SV rises, and the contour plot (Figure 2, IP vs. SV) similarly indicates lower roughness at higher servo voltages. This outcome concurs with prior findings that increasing the servo reference voltage yields lower surface roughness by maintaining a more stable spark gap [26]. In fact, among the five factors under consideration, servo voltage and discharge current exhibited the strongest individual impacts on Ra (Figure 4), suggesting that both the electrical energy per spark and the gap conditions are critical to surface finish. The 3D response surface for Ra (Figure 7)

illustrates these effects in combination, depicting a valley of minimal Ra at low IP and high SV (mild sparks, large gap) versus a peak of roughness at high IP and low SV (intense sparks, tight gap). In summary, the results indicate that achieving a smooth surface (low Ra), is best accomplished by using lower discharge energy (IP, Ton) and a sufficiently relaxed amplitude cycle and gap setting (higher Toff and SV). Conversely, pursuing for maximum material removal (high IP, long Ton, high amplitude) tends to result in a rougher the surface.

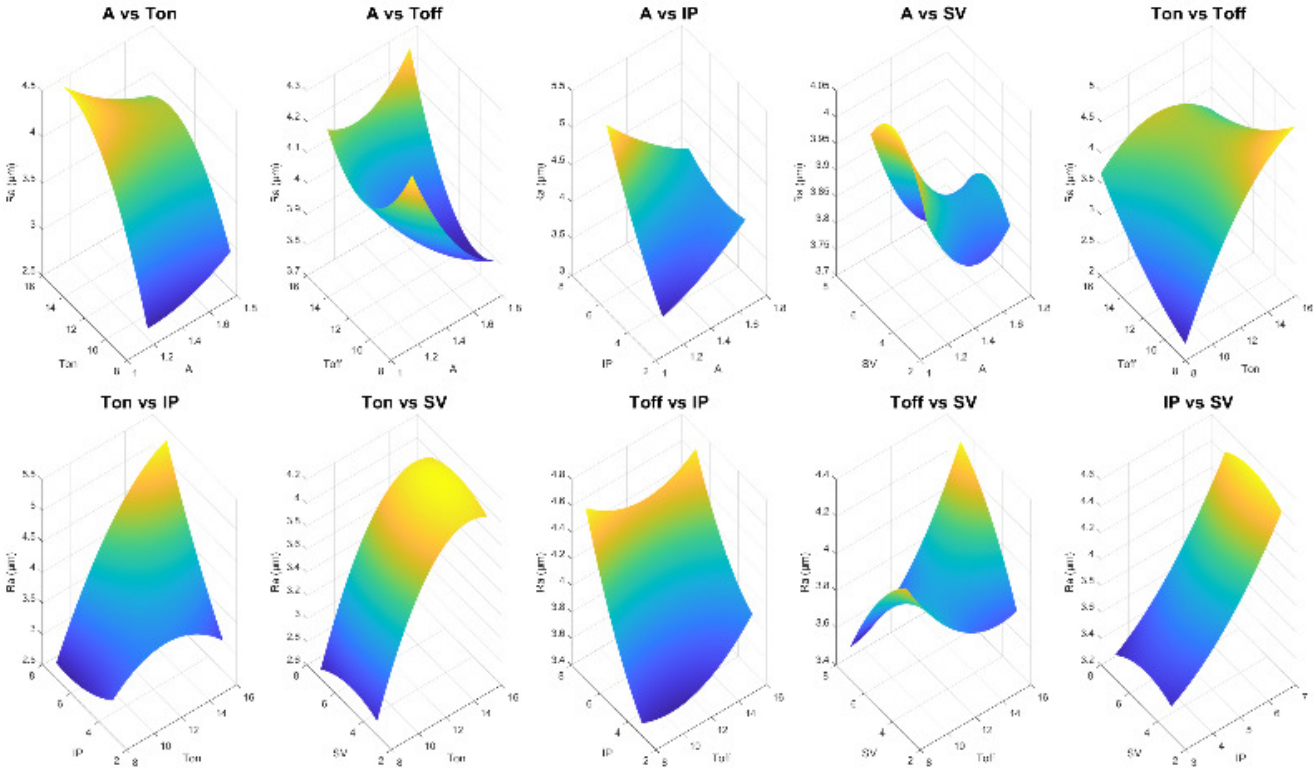

Fig. 7. 3D surface plots of input parameters on Ra.

It is noteworthy that the ultrasonic vibration assistance had a generally positive effect on surface quality in this study. Despite the higher MRR obtained, the Ra values did not degrade as severely as one might expect from more aggressive cutting conditions. The continuous shaking of the tool and/or workpiece by the ultrasonic vibration likely contributed to the removal of molten material and micro debris from the surface before their solidification as asperities, thereby preventing excessive surface roughening. Some prior researchers have cautioned that ultrasonic assistance can sometimes increase surface roughness, due to intensified discharges and micro-jet impacts on the surface [25]. For example, authors in [25] observed an approximate 10% rise in Ra when applying ultrasonic vibration in EDM of tungsten carbide, attributing it to the more intense plasma and jet forces in the spark gap. In this work, however, no such detrimental effect on Ra was observed; on the contrary, at optimal settings the ultrasonic-assisted process produced a slightly better (lower) roughness than similar conditions would in conventional EDM. This finding indicates that the benefits of ultrasonic vibration, such as its capacity to stabilize the discharge and remove debris, outweighed any tendency to increase crater size. Indeed, other studies have found that ultrasonic vibration can improve surface finish. For instance, authors in [27] reported that adding ultrasonic vibration in Wire-EDM reduced the surface roughness compared to the conventional process [27]. Our findings support this latter perspective: ultrasonic assistance, when properly tuned with the right EDM parameters, can simultaneously enhance MRR and maintain or improve surface quality.

C. Interaction Effects between Parameters

Beyond the individual influences of each factor, the experimental results reveal significant interaction effects among the input parameters, as illustrated by the interaction plots (Figure 8 for MRR and Figure 8 for Ra). Many factor pairs exhibit non-additive behavior, meaning the effect of one parameter on the outcome depends on the level of another parameter. For MRR, one of the strongest interactions observed is between the vibration amplitude (A) and the discharge current (IP). In the MRR interaction matrix (Figure 8), the lines representing MRR at low vs. high current are not parallel across different levels of vibration amplitude, indicating an interaction. Specifically, increasing IP yields a much larger MRR gain when the vibration amplitude is high (A at its high level) than when it is low. This implies that to fully leverage a higher discharge current, a sufficiently high amplitude cycle (short off-time) is required. Otherwise, long idle periods

between pulses waste the potential of the increased current. In practice, at low vibration amplitude the discharge frequency is limited, so even a high current cannot drastically raise MRR, In contrast, at high amplitude the combination of frequent and powerful discharges leads to a multiplicative improvement in MRR. This interaction underscores the importance of a balanced pulse regime: high current should be accompanied by frequent pulses to maximize material removal. Ultrasonic vibration further accentuates this beneficial synergy by keeping the gap clear at high pulse frequency. This allows for high-current, high-amplitude operation without the usual issue of debris-caused shorting, thus amplifying the combined effect of IP and amplitude on MRR.

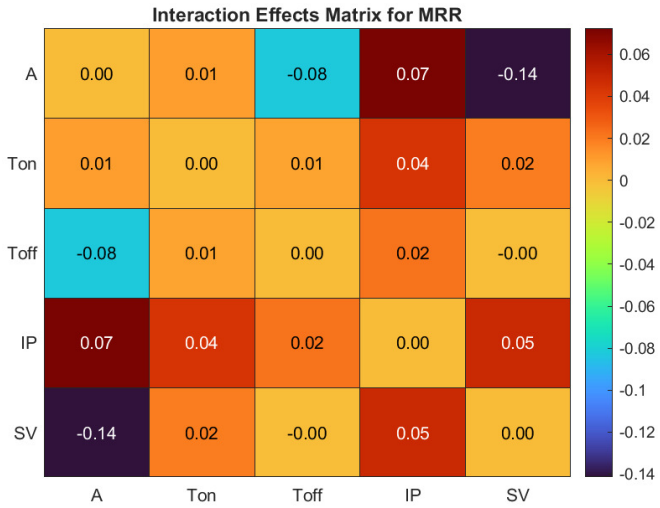

Fig. 8. Heatmap interaction plot of input parameters on MRR.

Another notable interaction is between pulse-on time (Ton) and pulse-off time (Toff). These two factors are inherently linked through the amplitude cycle, so it is unsurprising that their interaction influences the outcomes. The MRR interaction plot (Figure 8) shows that the effect of increasing Ton depends on the Toff setting. When Toff is short (high amplitude cycle), extending Ton significantly raises MRR. Essentially, the machine spends more time actively eroding material and does so frequently. However, when Toff is long (low amplitude cycle), the marginal benefit of a longer Ton is smaller; a significant portion of the cycle is spent waiting, so extremely long discharges yield diminishing returns as the electrolyte fully recovers each time. The results of the study demonstrate that MRR increases with Ton more steeply at low Toff than at high Toff, thereby confirming the aforementioned interaction. This finding is consistent with the need to adjust pulse duration and vibration amplitude in a coordinated manner. An optimal combination of these parameters (e.g. moderately long Ton with moderately short Toff) can outperform extreme settings that are inappropriate for either parameter. Ultrasonic assistance once again plays a pivotal role by permitting shorter Toff (higher amplitude) without the occurrence of instability, thereby allowing the use of longer Ton for greater MRR without incurring as many harmful arcs.

The interaction between discharge current (IP) and servo voltage (SV) is also significant, particularly for MRR. As illustrated in Figure 5, the impact of IP on MRR is modulated by the servo setting. Specifically, at a high SV, an increase in current results in a greater MRR increase compared to a low SV. When SV is low (a tighter gap), the gap may become choked with debris or experience more short-circuits at high current. Consequently, the full benefit of the increased discharge energy is not realized – the MRR curve flattens at high IP under low SV conditions. In contrast, at a higher SV (wider gap and more responsive servo control), the process can accommodate the higher current with fewer abnormal discharges, resulting in a steeper MRR rise with IP. This IP–SV interaction suggests that an aggressive electrical setting (high current) should be paired with an appropriately high servo voltage (looser gap control) to maintain stability and maximize MRR. It also highlights an important point for ultrasonic EDM: the ultrasonic vibration helps to mitigate the negative effects of a tight gap by expelling debris, effectively performing a similar role to increasing SV. Thus, in ultrasonic-assisted EDM, even at lower servo voltage settings, the gap is kept cleaner, which may reduce the severity of the IP–SV interaction compared to conventional EDM. In our case, we still found IP and SV to interact; however ultrasonic flushing likely made the process less sensitive to servo setting than it would otherwise be.

Regarding surface roughness (Figure 9), the interactions often mirror those observed in MRR but in terms of quality degradation. A strong interaction was observed between IP and Toff/on Ra. In the case of a short Toff (high amplitude), increasing the current from low to high caused a drastic rise in Ra, with the surface transitioning from a relatively smooth to a noticeably rough state. Conversely, at long Toff (plenty of cooling time), the effect of the current on surface roughness was less extreme. This suggests that the adverse effects of high current on surface finish are intensified under conditions of too frequent pulses (insufficient off-time). Debris and molten material accumulate with successive high-energy discharges, leading to large spatter and craters. However, in scenarios where the off-time is substantial, even a high current discharge has sufficient time to dissipate heat and eject melt before the next pulse, moderating the roughness increase. Thus, the combination of high IP and high amplitude is especially damaging to surface quality (much more so than either alone), as evidenced by the steep jump in Ra in that corner of the parameter space (Figures 3 and 7).

Similarly, an interaction between IP and SV is observed for Ra: at low SV (small gap), raising the current greatly increases roughness because the sparks occur in close proximity with more plasma confinement and residual debris. Conversely, at high SV, the roughness vs. current curve is flatter – a larger gap cushions the effect of higher current. In other words, a higher servo voltage can somewhat offset the roughness penalty of a high current by maintaining stability, an interaction inverse to the MRR case. Interactions between Ton and Toff also affect Ra: long pulses are especially harmful to surface finish if the off-time is too short to allow full crater cooling, leading to overlapping thermal damage. Our results (Figure 7) show Ra is highest when combining a long Ton with a short Toff, whereas

a long Ton with a long Toff yields much less roughness. This again emphasizes that no single parameter acts in isolation, and a balance is needed to avoid compounding negative effects on surface integrity.

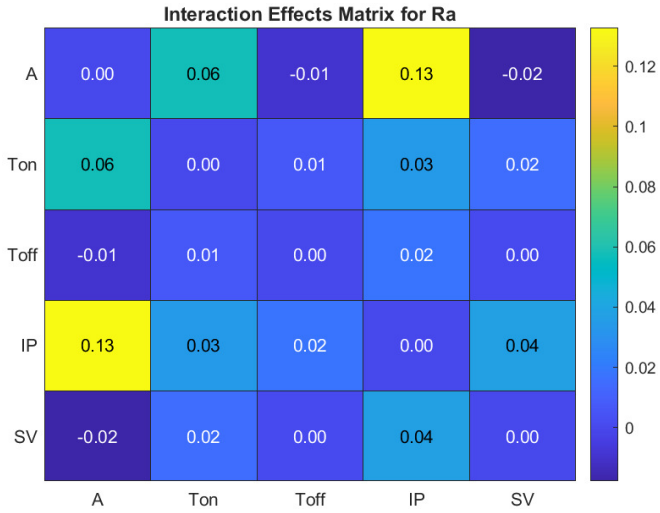

Fig. 9. Heatmap interaction plot of input parameters on Ra.

Overall, the interaction analysis highlights that optimizing ultrasonic EDM is not as simple as maximizing each factor independently; certain combinations must be managed to achieve the best outcomes. The interaction plots provided the necessary guidance, as they revealed the points at which lines deviated from parallel. Importantly, the presence of ultrasonic vibration in our process altered some interaction behaviors compared to conventional EDM reported in the literature. Many interactions that normally would be highly constraining (such as the current vs. amplitude trade-off for surface finish) are less severe here because ultrasonic agitation improves the flushing and stability. This implies that ultrasonic assistance expands the feasible processing window, enabling the manipulation of parameters with greater intensity without encountering the same level of detrimental interactions (e.g., uncontrollable roughness or tool wear). These findings underscore the advantage of the hybrid ultrasonic-EDM approach, which not only increases the main effects (higher MRR) but also moderates negative interactions between parameters, contributing to a more robust and optimal performance envelope.

D. Comparison with Previous Studies and Role of Ultrasonic Vibration

The results of the present study support and extend the findings from prior research in the field of EDM. In terms of general EDM parameter effects, our observations are in strong agreement with the established literature. The significance of discharge current and pulse duration in controlling MRR and surface roughness has been well documented. Numerous studies have identified current and Ton as the most influential factors on EDM performance metrics [24]. The findings of this study demonstrate that high current and long pulses yield higher MRR; however, this is achieved at the expense of a rougher surface. Conversely, lower energy settings produce smoother finishes. It was also determined that increasing the pulse-off time improves surface finish, and that raising the servo voltage can reduce roughness. These findings are consistent with those from earlier research in both die-sinking and Wire-EDM, which demonstrated that adequate flushing time and gap control lead to better surface quality [24, 26]. Therefore, with regard to conventional EDM aspects, our results reinforce the consensus understanding (e.g., higher spark energy → higher MRR and Ra, improved gap conditions → lower Ra).

More interestingly, this study provides insight into the effects of UV-EDM in comparison to previous works. The addition of ultrasonic vibration has been reported by many researchers to enhance machining performance, but with some differing observations on surface quality. Generally, there is agreement that ultrasonic assistance substantially increases MRR [25]. Our achieved MRR gains are in line with those reported in the literature. For instance, a review by the authors in [25] noted that ultrasonic vibration typically improves MRR by 20–70% depending on the conditions, and that applying ultrasonic vibration to the EDM tool boosted MRR by around 71% in their experiments. These improvements can be attributed to the more effective debris evacuation and higher stable discharge frequency enabled by ultrasonic vibration, as our results also demonstrated. In fact, the present study confirms the mechanistic explanations offered in prior research: the ultrasonic-induced cavitation and pressure waves drive out debris and refresh the dielectric, which in turn allows more frequent ignition of sparks and prevents premature arcing [25]. This mechanism was clearly reflected in our process. We observed fewer stalls and a consistently active spark gap when ultrasonics were applied, which agrees with the improved machining stability reported by others for vibration-assisted EDM [25].

Nevertheless, the impact of ultrasonic assistance on surface roughness has been a subject of debate. Some earlier studies have reported that while MRR increases with ultrasonics, surface roughness can slightly worsen. For instance, a modest increase in Ra was identified when machining with ultrasonic vibration, and a 10% higher roughness was measured on a WC alloy with ultrasonic EDM compared to conventional EDM [25]. It was explained that the intensified discharge energy and micro-jet impact in ultrasonic EDM can enlarge crater size, thus raising Ra [25]. It has also been identified that ultrasonic assistance alone leads to higher roughness unless combined with auxiliary techniques [25]. Our findings provide a nuanced perspective on this issue. We did observe the tendency for aggressive settings to produce rougher surfaces; however, we were able to mitigate some of those effects using ultrasonic vibration. In contrast to the reports of roughness degradation, our optimized ultrasonic-assisted process achieved surface roughness on par with or better than conventional EDM at equivalent settings. This finding is consistent with the findings of several recent studies that suggest ultrasonic vibration can improve or at least maintain surface quality. For instance, authors in [27] demonstrated in Wire-EDM of tungsten carbide that the addition of ultrasonic vibration not only increased MRR but also reduced Ra, attributing the improvement to more

uniform and less arced discharges. Our results support these findings, demonstrating that the surface finish does not have to be compromised for enhanced MRR when ultrasonic assistance is employed. The key is that ultrasonic vibration helps avoid the conditions that typically cause surface damage (e.g., lingering debris, secondary discharges), thus enhancing surface integrity in a high-energy regime.

In summary, the results of this study are largely in agreement with the existing body of knowledge on EDM and UV-EDM, while also extending that knowledge by demonstrating the interplay of parameters under ultrasonic assistance. The paramount importance of discharge current and pulse timing on performance metrics was confirmed, and the significant elevation of machining efficiency by ultrasonic vibration was demonstrated. Importantly, we found that with proper parameter optimization, ultrasonic vibration can improve the material removal rate and surface roughness simultaneously, supporting the conclusions of some researchers [27] and countering the concerns of others who observed roughness trade-offs [25]. These findings underscore the contribution of ultrasonic vibration to machining performance, as it effectively pushes the performance frontier, allowing higher MRR without commensurate deterioration of surface quality. Therefore, UV-EDM proves to be a powerful approach to improve productivity and surface finish in tandem, building upon previous works [24-27] and offering a more comprehensive understanding of how each input parameter and their interactions can be harnessed in an optimized EDM process. The insights derived from this study can serve as a guide for practitioners, assisting them in selecting the most suitable parameter combinations to fully exploit the benefits of ultrasonic vibration in EDM, while effectively controlling the quality of the machined surface.

E. Regression Model and Predictive Analysis

To quantitatively model the relationship between process parameters and machining performance, second-order regression equations were developed for both surface roughness (Ra) and MRR using the Box–Behnken experimental dataset. These models incorporate linear, quadratic, and two-factor interaction terms to capture the complex behavior of the UV-EDM process. The coded regression equations are expressed as follows:

- Regression equation for Ra (with R^2= 0.7832):

$$\begin{aligned}\text{Ra} = {} & -5.18712 + 1.95848\text{A} + 1.16798\text{Ton} - \\ & 0.07686\text{Toff} + 0.06536\text{IP} - 0.21602\text{SV} + \\ & 0.85744\text{A}^2 - 0.02866\text{Ton}^2 + 0.01097\text{Toff}^2 + \\ & 0.03169\text{IP}^2 - 0.02110\text{SV}^2 - 0.19535\text{A.Ton} + \\ & 0.11295\text{A.Toff} - 0.68780\text{A.IP} - 0.05837\text{A.SV} - \\ & 0.03884\text{Ton.Toff} + 0.08245\text{Ton.IP} + \\ & 0.00220\text{Ton.SV} - 0.01182\text{Toff.IP} + \\ & 0.03860\text{Toff.SV} + 0.00406\text{IP.SV} \end{aligned} \quad (2)$$

- Regression equation for MRR (with R^2= 0.9866):

$$\begin{aligned}\text{Ra} = {} & -4.04941 - 4.67250\text{A} + 1.10200\text{Ton} - \\ & 0.10519\text{Toff} + 0.70976\text{IP} + 0.59481\text{SV} + \\ & 1.69344\text{A}^2 - 0.05842\text{Ton}^2 + 0.00428\text{Toff}^2 - \\ & 0.10200\text{IP}^2 - 0.02954\text{SV}^2 - 0.06428\text{A.Ton} + \\ & 0.01221\text{A.Toff} - 0.13049\text{A.IP} - 0.20757\text{A.SV} - \\ & 0.00192\text{Ton.Toff} + 0.10959\text{Ton.IP} + \\ & 0.01569\text{Ton.SV} - 0.00738\text{Toff.IP} + \\ & 0.00458\text{Toff.SV} - 0.05246\text{IP.SV} \end{aligned} \quad (3)$$

The R^2 value of 0.7832 for Ra indicates that the quadratic model can explain over 78% of the variability in surface roughness, which is acceptable given the inherent stochastic nature of surface formation in EDM processes. In contrast, the model for MRR yields an excellent fit (R^2 = 0.9866), confirming the deterministic dependence of material removal rate on electrical input parameters.

These regression models provide further insight into the underlying relationships between process parameters and output responses, complementing the graphical interpretations discussed earlier. Key findings include:

- For Ra, the positive coefficients of A and Ton confirm their roughness-increasing effects, whereas the negative coefficient of SV indicates that higher servo voltage contributes to a smoother surface. The strong negative interaction between A and IP (–0.68780) reinforces earlier conclusions that increasing vibration amplitude at high current can exacerbate crater formation unless carefully controlled.
- For MRR, Ton, IP, and SV have been shown to positive linear coefficients, highlighting their role in improving machining efficiency. In contrast, the large negative coefficient of A (–4.67250) and the strong positive quadratic term A^2 (+1.69344) suggest a nonlinear relationship between ultrasonic amplitude and material removal. This is consistent with earlier surface plots, where MRR improved only beyond a threshold amplitude and degraded at the extremes.

Both models exhibit meaningful interaction terms (e.g., Ton × IP for both responses), which confirm the interaction effects identified in the matrix heatmaps. The good agreement between regression predictions and experimental observations validates the suitability of these models for optimization and process prediction purposes.

The derived equations can thus be used as surrogate models for multi-objective optimization, sensitivity analysis, and real-time parameter adjustment in advanced UV-EDM applications.

V. CONCLUSION

The present investigated the effects of key electrical and mechanical parameters on the machining performance of Ultrasonic Vibration-Assisted Electrical Discharge Machining (UV-EDM) using a systematic experimental approach. A five-factor, three-level Box–Behnken Design (BBD) was employed to develop predictive models for both Material Removal Rate (MRR) and surface roughness (Ra). The experimental setup, featuring a high-precision Sodick A30 EDM machine integrated with a 20 kHz ultrasonic vibration system, enabled a comprehensive exploration of the UV-EDM process space under controlled conditions.

The main conclusions derived from this research are summarized as follows:

- Discharge current (IP), pulse-on time (Ton), and ultrasonic vibration amplitude (A) have been identified as the most influential parameters affecting MRR and Ra. An increase in IP and Ton improves MRR, but it also leads to a degradation in surface finish. Conversely, higher servo voltage (SV) contributes to smoother surfaces without significantly compromising MRR.
- Ultrasonic vibration amplitude (A) demonstrates a nonlinear influence on both performance indicators. While moderate amplitudes enhance flushing efficiency and discharge stability, leading to improved MRR and reduced surface roughness, excessively high amplitudes can deteriorate surface quality, particularly at high discharge currents.
- The regression models developed for MRR and Ra effectively captured both main and interaction effects, with key interactions such as A × IP and Ton × IP significantly shaping the response behavior. The models provide valuable predictive capability for selecting optimal machining conditions.
- The interaction analysis and contour plots confirmed that the optimal process window for UV-EDM lies in the moderate-to-high range of Ton, SV, and IP, combined with optimized ultrasonic vibration amplitude (A). This combination balances debris removal, spark stability, and thermal impact on the surface.
- Compared with conventional EDM, the utilization of ultrasonic vibration significantly increased MRR while maintaining or improving surface finish, confirming its potential to overcome traditional trade-offs in EDM machining. These findings align with and extend prior research on ultrasonic-assisted EDM, highlighting its effectiveness in processing hard tool steels such as 90CrSi.

Overall, this study contributes to the understanding and optimization of UV-EDM processes, providing both experimental evidence and analytical tools for improving efficiency and surface integrity in precision machining applications. Future work may explore the implementation of adaptive control strategies based on these models, as well as the integration of real-time vibration monitoring to further enhance process reliability.

ACKNOWLEDGMENT

This work received funding from Project B2023-TNA-19, which is supported by the Ministry of Education and Training of Vietnam (MOET).

REFERENCES

[1] M. Hadad, L. Q. Bui, and C. T. Nguyen, "Experimental investigation of the effects of tool initial surface roughness on the electrical discharge machining (EDM) performance," *The International Journal of Advanced Manufacturing Technology*, vol. 95, no. 5, pp. 2093–2104, Mar. 2018, https://doi.org/10.1007/s00170-017-1399-2.

[2] M. K. Das, K. Kumar, T. Kr. Barman, and P. Sahoo, "Application of Artificial Bee Colony Algorithm for Optimization of MRR and Surface Roughness in EDM of EN31 Tool Steel," *Procedia Materials Science*, vol. 6, pp. 741–751, Jan. 2014, https://doi.org/10.1016/j.mspro.2014.07.090.

[3] M. K. Pradhan and C. K. Biswas, "Multi-response optimisation of EDM of AISI D2 tool steel using response surface methodology," *International Journal of Machining and Machinability of Materials*, vol. 9, no. 1/2, 2011, Art. no. 66, https://doi.org/10.1504/IJMMM.2011.038161.

[4] I. Puertas and C. J. Luis-Pérez, "Modelling of Surface Roughness (Ra and Rq) in the EDM of Reaction-Bonded Silicon Carbide," *Materials Science Forum*, vol. 526, pp. 151–156, Oct. 2006, https://doi.org/10.4028/www.scientific.net/MSF.526.151.

[5] M. Antar, P. Hayward, J. Dunleavey, and P. Butler-Smith, "Surface Integrity Evaluation of Modified EDM Surface Structure," *Procedia CIRP*, vol. 68, pp. 308–312, Jan. 2018, https://doi.org/10.1016/j.procir.2017.12.069.

[6] B. Jabbaripour, M. H. Sadeghi, Sh. Faridvand, and M. R. Shabgard, "Investigating the Effects of EDM Parameters on Surface Integrity, MRR and TWR in Machining of Ti–6Al–4V," *Machining Science and Technology*, vol. 16, no. 3, pp. 419–444, Jul. 2012, https://doi.org/10.1080/10910344.2012.698971.

[7] M. K. Pradhan and C. K. Biswas, "Modelling of machining parameters for MRR in EDM using response surface methodology," in *Proceedings of National Conference on Mechanism Science and Technology: from Theory to Application*, Hamirpur, India, 2008, pp. 535–542.

[8] M. K. Das, K. Kumar, T. K. Barman, and P. Sahoo, "Optimization of Surface Roughness and MRR in EDM Using WPCA," *Procedia Engineering*, vol. 64, pp. 446–455, Jan. 2013, https://doi.org/10.1016/j.proeng.2013.09.118.

[9] P. Zhang *et al.*, "Investigating mechanisms of debris removal in ultrasonic vibration-assisted EDM drilling," *International Journal of Mechanical Sciences*, vol. 279, Oct. 2024, Art. no. 109486, https://doi.org/10.1016/j.ijmecsci.2024.109486.

[10] P. Zhang, Z. Yin, C. Dai, Z. Cao, Q. Miao, and K. Zhang, "The effect of ultrasonic amplitude on the performance of ultrasonic vibration-assisted EDM micro-hole machining," *The International Journal of Advanced Manufacturing Technology*, vol. 122, no. 3, pp. 1513–1524, Sep. 2022, https://doi.org/10.1007/s00170-022-09852-3.

[11] J. Han, X. Gao, Y. Zhou, Z. Li, M. Gao, and Q. Zhang, "Machining characteristics in ultrasonic vibration-assisted powder-mixed electrical discharge machining of TiN ceramics," *Ceramics International*, vol. 50, no. 8, pp. 13478–13489, Apr. 2024, https://doi.org/10.1016/j.ceramint.2024.01.260.

[12] J. Singh, R. S. Walia, P. S. Satsangi, and V. P. Singh, "FEM modeling of ultrasonic vibration assisted workpiece in EDM process," *International Journal of Mechanics and Systems Engineering*, vol. 1, no. 1, pp. 8–16, Jan. 2011.

[13] V. D. Bui *et al.*, "Ultrasonic Vibration assisted Silver Integration by Powder Mixed EDM for Antibacterial Surfaces," *Procedia CIRP*, vol. 123, pp. 410–415, Jan. 2024, https://doi.org/10.1016/j.procir.2024.05.072.

[14] W. Chenxue, T. Sasaki, and A. Hirao, "Observation of Bubble Behavior in EDM with Ultrasonic Vibration," *Procedia CIRP*, vol. 113, pp. 267–272, Jan. 2022, https://doi.org/10.1016/j.procir.2022.09.157.

[15] Z. Li, J. Tang, Y. Li, and J. Bai, "Investigation on surface integrity in novel micro-EDM with two-dimensional ultrasonic circular vibration (UCV) electrode," *Journal of Manufacturing Processes*, vol. 76, pp. 828–840, Apr. 2022, https://doi.org/10.1016/j.jmapro.2022.03.004.

[16] Z. Li, J. Tang, and J. Bai, "A novel micro-EDM method to improve microhole machining performances using ultrasonic circular vibration (UCV) electrode," *International Journal of Mechanical Sciences*, vol. 175, Jun. 2020, Art. no. 105574, https://doi.org/10.1016/j.ijmecsci.2020.105574.

[17] Y.-C. Lin, J.-C. Hung, H.-M. Chow, A.-C. Wang, and J.-T. Chen, "Machining Characteristics of a Hybrid Process of EDM in Gas Combined with Ultrasonic Vibration and AJM," *Procedia CIRP*, vol. 42, pp. 167–172, Jan. 2016, https://doi.org/10.1016/j.procir.2016.02.213.

[18] D. Kremer, C. Lhiaubet, and A. Moisan, "A Study of the Effect of Synchronizing Ultrasonic Vibrations with Pulses in EDM," *CIRP Annals*, vol. 40, no. 1, pp. 211–214, Jan. 1991, https://doi.org/10.1016/S0007-8506(07)61970-2.

[19] G. S. Prihandana, M. Mahardika, M. Hamdi, Y. S. Wong, and K. Mitsui, "Effect of micro-powder suspension and ultrasonic vibration of dielectric fluid in micro-EDM processes—Taguchi approach," *International Journal of Machine Tools and Manufacture*, vol. 49, no. 12–13, pp. 1035–1041, Oct. 2009, https://doi.org/10.1016/j.ijmachtools.2009.06.014.

[20] T. P. T. Le, V. T. Dinh, T. Q. D. Nguyen, D. B. Vu, and T. T. Vu, "Application of the Multi-Criteria Decision Method to Find the Best Input Factors for Electrical Discharge Machining 90CrSi Tool Steel using Graphite Electrodes," *Engineering, Technology & Applied Science Research*, vol. 14, no. 6, pp. 18883–18888, Dec. 2024, https://doi.org/10.48084/etasr.9114.

[21] S. K. Ghazi, M. A. Abdullah, and H. H. Abdulridha, "Investigating the Impact of EDM Parameters on Surface Roughness and Electrode Wear Rate in 7024 Aluminum Alloy," *Engineering, Technology & Applied Science Research*, vol. 15, no. 1, pp. 19401–19407, Feb. 2025, https://doi.org/10.48084/etasr.9252.

[22] R. H. Myers, D. C. Montgomery, and C. M. Anderson-Cook, *Response Surface Methodology: Process and Product Optimization Using Designed Experiments*, 4th ed. Hoboken, NJ, USA: Wiley, 2016.

[23] D. C. Montgomery, *Design and Analysis of Experiments*, 9th ed. Hoboken, NJ, USA: Wiley, 2017.

[24] S. Daneshmand, E. F. Kahrizi, and M. M. Ghahi, "Investigation of EDM Parameters on Surface Roughness and Material Removal Rate of NiTi60 Shape Memory Alloys," *Australian Journal of Basic and Applied Sciences*, vol. 6, no. 12, pp. 218–225, Nov. 2012.

[25] N. Sabyrov, M. P. Jahan, A. Bilal, and A. Perveen, "Ultrasonic Vibration Assisted Electro-Discharge Machining (EDM)—An Overview," *Materials*, vol. 12, no. 3, Feb. 2019, Art. no. 522, https://doi.org/10.3390/ma12030522.

[26] H. Singh, K. Goyal, and P. Kumar, "Experimental Investigation of WEDM Variables on Surface Roughness of AISI H13," *Manufacturing Science and Technology*, vol. 1, no. 2, pp. 23–30, Nov. 2013, https://doi.org/10.13189/mst.2013.010201.

[27] A. Muttamara and P. Nakwong, "Enhancing Wire-EDM Performance with Zinc-Coated Brass Wire Electrode and Ultrasonic Vibration," *Micromachines*, vol. 14, no. 4, Apr. 2023, Art. no. 862, https://doi.org/10.3390/mi14040862.